Modelling Water Wave Overwash of a Sea Ice Floe

David Skene[1], Luke Bennetts[1,†], Michael Meylan[2], Alessandro Toffoli[3] and Jason Monty[4]

[1]School of Mathematical Sciences, University of Adelaide, 5005 Australia
[2]School of Mathematical and Physical Sciences, University of Newcastle, 2308 Australia
[3]Centre for Ocean Engineering Science and Technology, Swinburne University of Technology, 3122 Australia
[4]School of Mechanical Engineering, University of Melbourne, 3010 Australia
[†]luke.bennetts@adelaide.edu.au

Highlights

· Experimental validation of a mathematical model of wave-induced flexural motion of a thin floating plate.
· First model of wave overwash of an ice floe, which is validated by laboratory measurements.

Introduction

Mathematical models of ocean surface waves travelling through the sea ice covered ocean and impacting the ice cover have been developed for over 40 years now. The kernel of the models is a model of water waves interacting with a solitary ice floe. The ice floe is conventionally modelled as thin floating elastic plate. Water motions are conventionally modelled using potential flow theory.

Moreover, linear motions are assumed. However, as the floe has a small freeboard, incident waves of modest amplitudes are easily able to overwash the floe (run over its upper surface). The presence of overwash violates the assumption that motions are small perturbations from the equilibrium, which undergirds linear theory.

The impact of overwash on the motions of the floe and the surrounding wave field have not been investigated previously. More fundamentally, few attempts have been made to validate the linear thin-plate/potential-flow model.

In one notable exception, Montiel *et al.* (2013*a*,*b*) conducted a series of laboratory wave tank experiments to study the flexural motion of a floating thin plastic disk, as a model ice floe. They showed the linear model was able to predict the motions accurately. However, they attached a barrier to the edge of the model floe to prevent overwash in the experiments. Subsequently, their results provide no information on the impacts of overwash.

Results of a new series of wave tank experiments are reported here. In the experiments, no edge barrier was used and the incident waves were able to overwash the floe. The experimental measurements are used to show the linear model is able to predict the motions of the floe accurately, and, hence, that overwash does not significantly affect floe motions for the chosen parameter range.

This finding is used as the basis of a mathematical model of a wave overwashing an ice floe. The model is validated by measurements of the overwash depth recorded during the experiments. The model-data comparison shows generally very pleasing agreement and indicates the limit of validity of the model.

Experimental model

Experimental models of water waves interacting with an ice floe were implemented at the Mitchell Hydrodynamics Laboratory, University of Melbourne, Australia, and the Coastal Ocean and Sediment Transport (COAST) laboratories, Plymouth University, U.K. The models investigated one- and two-dimensional wave motions, respectively. The latter model is described here, and a selection of corresponding results is presented.

A thin plastic plate was installed in the COAST wave basin, as a model ice floe, on water of depth $H = 0.5\,\mathrm{m}$. The floe was loosely moored. Two different plastics, with distinct material properties, were used. First, a relatively dense and rigid polypropylene plastic, with a manufacturer specified density of $\rho_{\mathrm{pl}} = 905\,\mathrm{kg\,m^{-3}}$ and Young's modulus $E = 1600\,\mathrm{MPa}$. Second, a relatively light and compliant polyvinyl chloride (PVC) plastic with density $\rho_{\mathrm{pl}} = 500\,\mathrm{kg\,m^{-3}}$ and Young's modulus $E = 500\,\mathrm{MPa}$. Both plastics were provided with thicknesses $D = 5\,\mathrm{mm}$ and $10\,\mathrm{mm}$, and $20\,\mathrm{mm}$ and $40\,\mathrm{mm}$ (polypropylene) and $19\,\mathrm{mm}$ (PVC). The plates were cut into squares with side lengths $2L = 1\,\mathrm{m}$.

A series of tests were conducted in which the model floes were set in motion by regular incident waves. The motions were recorded stereoscopically by the Qualysis motion tracking system. Wave periods $T = 0.6\,\mathrm{s}$, $0.8\,\mathrm{s}$ and $1\,\mathrm{s}$ were used for the incident waves. The corresponding wavelengths are $0.56\,\mathrm{m}$, $1\,\mathrm{m}$ and $1.51\,\mathrm{m}$, respectively, i.e. approximately half

the floe length, equal to the floe length and 1.5 times the floe length. Four incident wave steepnesses were tested: $ka = 0.04$, 0.08, 0.1 and 0.15, where k and a denote the incident wave number and amplitude, respectively.

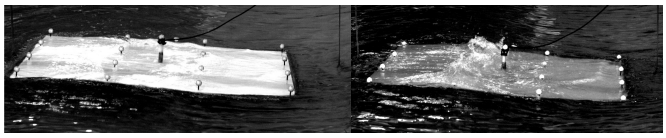

Figure 1: Photos of mild and severe overwash.

A small gauge was deployed in the middle of the upper surface of the floe to measure the depth of overwashed fluid. Overwash occurred in approximately 60% of the cases tested. The polypropylene floes, which have a relatively small freeboard, experienced the strongest overwash.

Figure 1 shows photos of overwash occurring in the tests. The left-hand panel shows mild overwash occurring for a 10 mm thick PVC floe and a 1 s period incident wave with steepness 0.15. A bore wave is visible in the shallow overwash. Bores are typical when overwash occurs. The right-hand panel shows severe overwash occurring for a 10 mm thick polypropylene floe and a 1 s period incident wave with steepness 0.15. In this case bore waves travelling up and down the plate have collided and, subsequently, caused breaking.

For each test conducted, the recorded flexural motions of the floe are converted into a spectral representation via a decomposition into the floe's natural modes of vibration. Thus, let $\eta_m(t)$ denote the vertical displacement of the mth marker. After the initial transients have passed, the signal is approximately periodic in time at the angular frequency of the incident wave, ω. Therefore, a complex amplitude A_m is calculated such that $\eta_m(t) \approx \mathrm{Re}\{A_m \mathrm{e}^{-\mathrm{i}\omega t}\}$, using least-squares minimization.

Horizontal locations on the surface of the floe are define by a Cartesian coordinate system (x, y). The origin of the coordinate system is the geometric center of the floe. The x coordinate points in the direction of the incident wave.

The floe's orthonormal natural modes of vibration are denoted $w_j(\mathbf{x})$, where $\mathbf{x} = (x, y)$. Following Kirchoff-Love thin-plate theory the modes satisfy the governing equation

$$\Delta^2 w_j = \lambda_j^4 w_j,$$

where λ_j are eigenvalues, plus free-edge conditions. They are calculated using the finite element method outlined by Meylan (2002).

The complex amplitudes A_m are projected onto a finite-dimensional space spanned by the dominant natural modes of vibration, i.e.

$$A_m \approx \sum_{j\in\Lambda} \xi_j^{\mathrm{ex}} w_j(\mathbf{x}_m)$$

where $\mathbf{x}_m$ denotes the location of the mth marker. The set $\Lambda = \{1, 2, 5, 6, 7, 9, 11\}$ contains indices of the modes used for computations. Only motions symmetric with respect to the direction of the incident wave are considered. The first two modes represent the rigid body motions of the floe: heave and pitch, respectively. The final five modes represent the primary flexural motions. The weights ξ_j^{ex} are obtained via a least squares minimization routine.

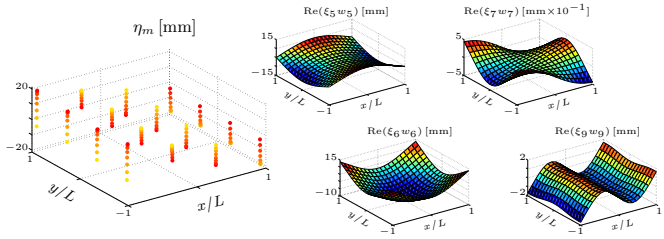

Figure 2: Motion of floe markers (left), and corresponding four dominant flexural modes (right).

Figure 2 shows an example decomposition of the floe motion into the natural modes. The example is for a 5 mm thick polypropylene floe, and a 0.8 s period incident wave with steepness 0.1. The left-hand panel shows the recorded vertical displacements of the markers over a short time interval. The right-hand panels show the corresponding four dominant weighted flexural modes.

Linear mathematical model

Following potential flow theory and assuming time-harmonic conditions, the water's velocity field is defined by the gradient of the scalar velocity potential $\mathrm{Re}\{\phi(x, y, z)\mathrm{e}^{-\mathrm{i}\omega t}\}$. Locations in the water are defined by the Cartesian coordinate system (x, y, z), where $\mathbf{x} = (x, y)$ defines horizontal locations and z is the vertical coordinate. The time-independent component of the velocity potential, ϕ, satisfies Laplace's equation throughout the water domain, i.e.

$$\Delta\phi = 0 \quad \text{for} \quad \mathbf{x} \in \mathbb{R}^2 \quad \text{and} \quad -H < z < 0, \quad \text{(1a)}$$

and a zero normal flow bed condition

$$\phi_z = 0 \quad \text{for} \quad \mathbf{x} \in \mathbb{R}^2 \quad \text{and} \quad z = -H. \quad \text{(1b)}$$

On the linearised water surface away from the floe, the potential satisfies the free-surface condition

$$\phi_z = \frac{\omega^2}{g}\phi \quad \text{for} \quad \mathbf{x} \notin \Omega \quad \text{and} \quad z = 0. \quad \text{(1c)}$$

On the linearised interface between the water surface and the underside of the floe, the potential is coupled

to the floe motion via kinematic and dynamic conditions, respectively

$$\phi_z = -\mathrm{i}\omega \sum_{j=1}^{\infty} \xi_j^{\mathrm{ma}} w_j \qquad \text{and} \tag{1d}$$

$$\frac{\mathrm{i}\omega}{g}\phi = \sum_{j=1}^{\infty} \left(1 + \beta\lambda_j^4\right) \xi_j^{\mathrm{ma}} w_j - \omega^2 \gamma \sum_{j=1}^{\infty} \xi_j^{\mathrm{ma}} w_j, \tag{1e}$$

Here, $\gamma = \rho_{\mathrm{pl}} D/\rho g$ is the scaled mass of the floe and $\beta = ED^3/\{12(1-\nu^2)\rho g\}$ is the scaled flexural rigidity, where $\nu = 0.4$ (polypropylene floes) and 0.3 (PVC) are typical values of Poisson's ratio.

The velocity potential is expanded as

$$\phi = \phi^{\mathrm{I}} + \phi^{\mathrm{D}} - \mathrm{i}\omega \sum_{j=1}^{\infty} \xi_j^{\mathrm{ma}} \phi_j^{\mathrm{R}} \tag{2}$$

where ϕ^{I} is the incident wave potential with amplitude a. The sum of the incident wave and diffraction potentials, $\phi^{\mathrm{I}} + \phi^{\mathrm{D}}$, is the solution of the problem in which the floe is held in place, i.e. equations (1a–d) with $\xi_j^{\mathrm{ma}} = 0$ $(j = 1, 2, \dots)$. The radiation potentials, ϕ_j^{R} $(j = 1, 2, \dots)$ are solutions of the problems in which the floe oscillates in one of its degrees of freedom with unit amplitude, i.e. equations (1a–d) with $\xi_i^{\mathrm{ma}} = \delta_{ij}$ $(i = 1, 2, \dots)$. The diffraction and radiation potentials are calculated by using a Green's function to convert the boundary value problems to integral equations, which are solved numerically via a constant panel method (Meylan, 2002).

A linear system for the modal weights, ξ_j^{ma}, is obtained by applying the dynamic coupling condition (1e) to the expanded velocity potential (2) and taking inner-products with respect to the subset of the modes defined by Λ. The system is expressed is

$$\left(\mathbf{K} + \mathbf{C} - \omega^2\mathbf{M} - \omega^2\mathbf{A}(\omega) - \mathrm{i}\omega\mathbf{B}(\omega)\right)\boldsymbol{\xi}^{\mathrm{ma}} = \mathbf{f}(\omega).$$

Here $\mathbf{K}$, $\mathbf{C}$ and $\mathbf{M}$ are the stiffness, hydrostatic-restoring and mass matrices:

$$\mathbf{K} = \lceil \beta\lambda_j^4 \rfloor, \qquad \mathbf{M} = \gamma\mathbf{I} \qquad \text{and} \qquad \mathbf{C} = \mathbf{I},$$

where $\lceil \dots \rfloor$ denotes a diagonal matrix and $\mathbf{I}$ is the identity matrix. The real matrices $\mathbf{A}$ and $\mathbf{B}$ are known as the added-mass and damping matrices, respectively, and are defined element-wise by

$$\omega^2\mathbf{A}_{ij} + \mathrm{i}\omega\mathbf{B}_{ij} = \frac{\omega^2}{g} \iint_{\Omega} \phi_j^{\mathrm{R}}(\mathbf{x}, 0) w_i(\mathbf{x}) \, \mathrm{d}\mathbf{x}.$$

The forcing vector, $\mathbf{f}$, is defined by

$$\mathbf{f}_j = \frac{\mathrm{i}\omega}{g} \iint_{\Omega} \left(\phi^{\mathrm{I}}(\mathbf{x}, 0) + \phi^{\mathrm{D}}(\mathbf{x}, 0)\right) w_j(\mathbf{x}) \, \mathrm{d}\mathbf{x}.$$

The system is solved for the modal weights, which are contained in the vector $\boldsymbol{\xi}^{\mathrm{ma}}$.

Results

Figure 3 shows linear-model predictions of the magnitudes of the dominant modes and values calculated from the experimental data. The magnitudes of the modal amplitudes are scaled with respect to the incident amplitude, a. Results shown are for the polypropylene floes, which experience stronger overwash. The corresponding results for the PVC floes are consistent.

The experimental data indicate the floe's motion is, essentially, linear, i.e. the modal weights scale with the incident amplitude. Small discrepancies are notable for certain cases, for example, the 1 s period, 0.08 steepness incident waves for a 10 mm thick polypropylene floe. However, no consistent dependence is evident in those cases, and experimental errors are a probable cause of the discrepancies.

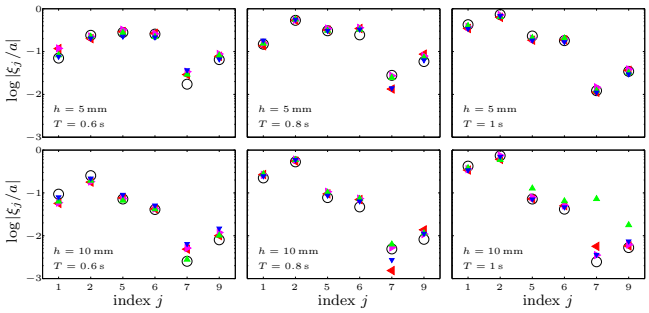

Figure 3: Comparisons of scaled modal weight magnitudes extracted from experimental data (triangles) and predicted by theoretical model for polypropylene floes (black circles). Incident steepnesses are: $ka = 0.04$ (blue, triangles down); 0.08 (green, up); 0.1 (magenta, right); and 0.15 (red, left).

The model is able to capture the magnitudes of the modal weights accurately. The model predictions are marginally more accurate for the thinner floes. Note that the logarithmic scale used to display the results emphasises errors for modal weights with small magnitudes. The model-data agreement found indicates that nonlinear phenomena inherent in wave-floe interactions, in particular, overwash, but also slamming and drift, have only a negligible effect on flexural motions.

Overwash model

The linear model is extended to a nonlinear model that incorporates overwash, by assuming:

(i) floe motions are governed by linear theory;

(ii) the height of the wave above the floe edges and its horizontal velocity forces overwash; and

(iii) overwash does not influence the surrounding wave field.

The model is two-dimensional (one horizontal dimension and one vertical dimension). Figure 6 shows an example snapshot of motions predicted by the model.

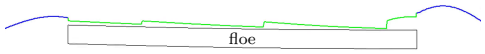

Figure 4: Overwash model: overwash fluid surface (green) and surrounding fluid surface (blue).

The overwashed fluid is modelled by the shallow-water equations, which, in conservative form, are

$$(h)_t + (hu)_x = 0 \qquad (3a)$$

$$\text{and} \qquad (hu)_t + (hu^2 + 1/2 * gh^2)_x = 0. \qquad (3b)$$

Here $h(x,t)$ is the depth of the overwashed fluid, $u(x,t)$ is the depth-averaged horizontal fluid velocity. Equations (3) account for the motion of the floe beneath the fluid. They are solved numerically using the finite volume method outlined in Kurganov & Tadmor (2000) and Kurganov *et al.* (2001) for spatial discretisation in conjunction with a total variation diminishing Runge-Kutta method for time stepping. The numerical scheme accurately resolves the bores produced by the shallow-water equations which is evident in figure 6.

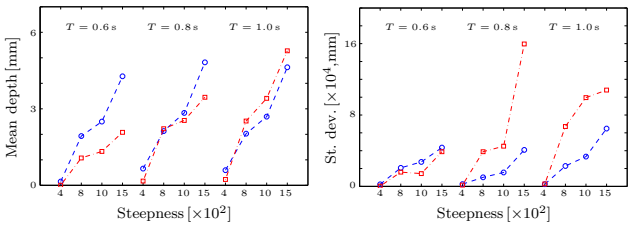

Figure 5: Comparisons of model overwash predictions (blue circles) with experimental data (red squares) for 5 mm thick polypropylene floes.

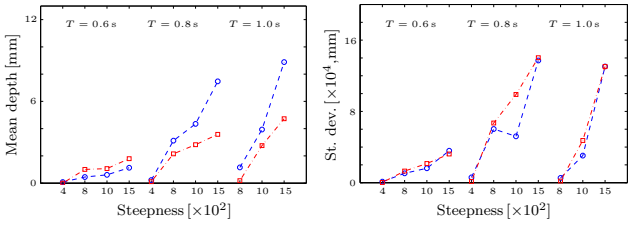

Figure 6: As in figure 5 but for a 10 mm thick floe.

Figures 5–6 show example comparisons of model predictions of the overwash depth mean and standard deviation at the centre of the floe and values calculated from the experimental data. Results are, again, for polypropylene floes.

In general:

- overwash becomes deeper as incident waves become steeper and the incident period increases;
- and overwash tends to be deepest for the thinner floes.

In terms of the model-data agreement:

- the model tends to slightly overestimate the mean depth and underestimate the standard deviation;
- the model is marginally more accurate for the polypropylene floes; and
- the model is least accurate for deep overwash (greater than approximately 5–6 mm), presumably because the model assumptions are no longer valid in the deep overwash regime.

Summary

1. A linear model accurately predicts the motions of a model floe induced by regular incident waves.
2. A relatively simple model, in which overwash is forced by the linear model, predicts mean overwash depth with pleasing accuracy.

Acknowledgements

The Universities of Plymouth, Melbourne and Newcastle funded the experiments. The Australian Antarctic Science Program funds DS and LB. The Australian Research Council funds LB and JM. The US Office of Naval Research funds MM.

References

Kurganov, A. & Tadmor, E. 2000 New high-resolution central schemes for nonlinear conservation laws and convectiondiffusion equations *J. Comp. Phys.* **160**, 241–282.

Kurganov, A., Noelle, S. & Petrova, G. 2001 Semidiscrete central-upwind schemes for hyperbolic conservation laws and Hamilton–Jacobi equations *SIAM J. Sci. Comput.* **23**, 707–740.

Meylan, M. H. 2002 Wave response of an ice floe of arbitrary geometry. *J. Geophys. Res.* **107**.

Montiel, F., Bonnefoy, F., Ferrant, P., Bennetts, L. G., Squire, V. A. & Marsault, P. 2013*a* Hydroelastic response of floating elastic disks to regular waves. Part 1: Wave tank experiments. *J. Fluid Mech.* **723**, 604–628.

Montiel, F., Bennetts, L. G., Squire, V. A., Bonnefoy, F. & Ferrant, P. 2013*b* Hydroelastic response of floating elastic disks to regular waves. Part 2: Modal analysis. *J. Fluid Mech.* **723**, 629–652.